

# Bifunctional Abietadiene Synthase: Free Diffusive Transfer of the (+)-Copalyl Diphosphate Intermediate between Two Distinct Active Sites

Reuben J. Peters,<sup>†</sup> Matthew M. Ravn,<sup>‡</sup> Robert M. Coates,<sup>‡</sup> and Rodney B. Croteau<sup>\*,†</sup>

Contribution from the Institute of Biological Chemistry, Washington State University, Pullman, Washington 99164-6340, and Department of Chemistry, University of Illinois, 600 South Matthews Avenue, Urbana, Illinois 61801

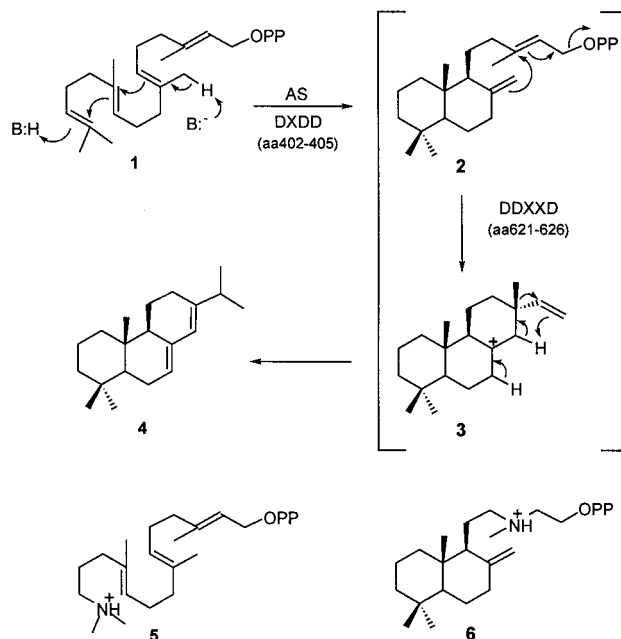
Received March 13, 2001

**Abstract:** Abietadiene synthase (AS) catalyzes two sequential, mechanistically distinct cyclizations in the conversion of geranylgeranyl diphosphate to a mixture of abietadiene double bond isomers as the initial step of resin acid biosynthesis in grand fir (*Abies grandis*). The first reaction converts geranylgeranyl diphosphate to the stable bicyclic intermediate (+)-copalyl diphosphate via protonation-initiated cyclization. In the second reaction, diphosphate ester ionization-initiated cyclization generates the tricyclic perhydrophenanthrene-type backbone, and is directly coupled to a 1,2-methyl migration that generates the C13 isopropyl group characteristic of the abietane family of diterpenes. Using the transition-state analogue inhibitor 14,15-dihydro-15-azageranylgeranyl diphosphate, it was demonstrated that each reaction of abietadiene synthase is carried out at a distinct active site. Mutations in two aspartate-rich motifs specifically delete one or the other activity and the location of these motifs suggests that the two active sites reside in separate domains. These mutants effectively complement each other, suggesting that the copalyl diphosphate intermediate diffuses between the two active sites in this monomeric enzyme. Free copalyl diphosphate was detected in steady-state kinetic reactions, thus conclusively demonstrating a free diffusion transfer mechanism. In addition, both mutant enzymes enhance the activity of wild-type abietadiene synthase with geranylgeranyl diphosphate as substrate. The implications of these results for the kinetic mechanism of abietadiene synthase are discussed.

## Introduction

The secretion of oleoresin (a roughly equal mixture of monoterpene olefins (turpentine) and diterpene resin acids (rosin)<sup>1</sup>) is the primary response of conifers to wounding, following which evaporation of the turpentine carrier results in crystallization and polymerization of the nonvolatile resin acids to seal the wound site.<sup>2</sup> Abietadiene synthase (AS) catalyzes the committed step of resin acid biosynthesis in grand fir (*Abies grandis*) by cyclization of the universal diterpene precursor geranylgeranyl diphosphate (GGPP, **1**) to a mixture of abietadiene double bond isomers, which are subsequently oxidized to the corresponding resin acids.<sup>3,4</sup> To produce the tricyclic perhydrophenanthrene (abietane) skeletal structure, AS carries out two consecutive, mechanistically distinct cyclizations (Scheme 1).<sup>4</sup> The first is initiated by protonation across the terminal 14,-15-double bond of GGPP, producing the stable bicyclic intermediate (+)-copalyl diphosphate [(+)-CPP, **2**], in a reaction analogous to that catalyzed by kaurene synthase A [(-)-copalyl diphosphate synthase, CPS] of the gibberellin biosynthetic pathway.<sup>5,6</sup> In the second cyclization mediated by AS, diphos-

**Scheme 1.** AS-Catalyzed Reactions and Aza Analogues of Carbocation Intermediates<sup>a</sup>



\* Corresponding author: (phone) (509) 335-1790; (fax) (509) 335-7643; (e-mail) croteau@wsu.edu.

<sup>†</sup> Washington State University.

<sup>‡</sup> University of Illinois.

(1) Lewinsohn, E.; Savage, T. J.; Gijzen, M.; Croteau, R. *Phytochem. Anal.* **1993**, *4*, 220–225.

(2) Phillips, M. A.; Croteau, R. B. *Trends Plant Sci.* **1999**, *4*, 184–190.

(3) LaFever, R. E.; Stofer Vogel, B. S.; Croteau, R. *Arch. Biochem. Biophys.* **1994**, *131*, 139–149.

(4) Peters, R. J.; Flory, J. E.; Jetter, R.; Ravn, M. M.; Lee, H.-J.; Coates, R. M.; Croteau, R. B. *Biochemistry* **2000**, *39*, 15592–15602.

<sup>a</sup> Aspartate-rich motifs involved in each cyclization reaction are also depicted; amino acid (aa) numbering is based on the preprotein (i.e. rAS starts with Met then Val 85 → Ala 868).

phate ester ionization of (+)-CPP (**2**) forms the third ring in a reaction corresponding to that mediated by kaurene synthase B

(kaurene synthase, KS).<sup>5,6</sup> However, in AS this cyclization is immediately coupled, via intramolecular proton transfer<sup>7</sup> within a sandaracopimarenyl intermediate (**3**),<sup>8</sup> to a 1,2-methyl migration that creates the C13 isopropyl group characteristic of abietanes, such as abietadiene (**4**).

Both native and recombinant AS (rAS)<sup>9</sup> are bifunctional in catalyzing both reactions, in contrast to the formation of (–)-kaurene in higher plants which requires the two distinct enzymes, CPS and KS.<sup>5,6</sup> However, an unrelated fungal bifunctional kaurene synthase (FCPS/KS) catalyzing both cyclizations has been identified and shown to contain two distinct active sites.<sup>10</sup> AS contains a DXDD motif conserved in CPS<sup>11</sup> and triterpene cyclases<sup>12,13</sup> that is involved in the protonation-initiated cyclization reaction, as well as a DDXXD motif also found in KS<sup>14</sup> and other terpene synthases<sup>15,16</sup> that is involved in diphosphate ionization-initiated cyclization. FCPS/KS contains similar motifs and mutation of either aspartate-rich motif prevents the corresponding cyclization.<sup>17</sup>

In the formation of kaurene, the intermediate (–)-CPP is channeled between CPS and KS, which form a functional heterodimer.<sup>6</sup> FCPS/KS also seems to exhibit intermediate channeling; (*E,E,E*)-geranylgeranyl diphosphate (GGPP) reacts to form kaurene at a faster rate than does (–)-CPP.<sup>17</sup> In this study, we demonstrate that AS also contains distinct active sites responsible for each cyclization step that are defined, at least in part, by the two respective aspartate-rich DXDD and DDXXD motifs. The location of these motifs in a modeled AS structure suggests that the two active sites reside in separate domains (see Figure 4), similar to the organization of FCPS/KS.<sup>17</sup> However, unlike the kaurene synthases, the (+)-CPP intermediate of AS is not channeled between the two active sites in this monomeric enzyme, but rather is transferred by a free diffusion mechanism. Previous kinetic analysis of AS demonstrated that the intrinsic rate-limiting step of the overall reaction resides after formation of (+)-CPP, although substrate inhibition prevents direct observation of this limiting step with GGPP as substrate.<sup>4</sup> Based in part on the mistaken assumption that FCPS/KS exhibited similar GGPP substrate inhibition,<sup>17</sup> we had suggested that nonproductive binding of GGPP at the second active site limited the overall reaction.<sup>4</sup> Here we demonstrate that GGPP inhibits its own cyclization, not that of (+)-CPP.

## Experimental Procedures

**Materials and General Procedures.** Liquid scintillation counting and product analysis by GC-MS were carried out as previously

(5) Saito, T.; Abe, H.; Yamane, H.; Sakurai, A.; Murofushi, N.; Takio, K.; Takahashi, N.; Kamiya, Y. *Plant Physiol.* **1995**, *109*, 1239–1245.

(6) Duncan, J. D.; West, C. A. *Plant Physiol.* **1981**, *68*, 1128–1134.

(7) Ravn, M. M.; Coates, R. M.; Jetter, R.; Croteau, R. *J. Chem. Soc., Chem. Commun.* **1998**, *1998*, 21–22.

(8) Ravn, M. M.; Coates, R. M.; Flory, J.; Peters, R. J.; Croteau, R. *Org. Lett.* **2000**, *2*, 573–576.

(9) Stofer Vogel, B.; Wildung, M. R.; Vogel, G.; Croteau, R. *J. Biol. Chem.* **1996**, *271*, 23262–23268.

(10) Kawaide, H.; Imai, R.; Sassa, T.; Kamiya, Y. *J. Biol. Chem.* **1997**, *272*, 21706–21712.

(11) Sun, T.-P.; Kamiya, Y. *Plant Cell* **1994**, *6*, 1509–1518.

(12) Poralla, K. In *Comprehensive Natural Products Chemistry: Isoprenoids Including Carotenoids and Steroids*; Cane, D. E., Ed.; Elsevier: Oxford, 1999; Vol. 2, pp 307–319.

(13) Abe, I.; Prestwich, G. D. In *Comprehensive Natural Products Chemistry: Isoprenoids Including Carotenoids and Steroids*; Cane, D. E., Ed.; Elsevier: Oxford, 1999; Vol. 2, pp 267–298.

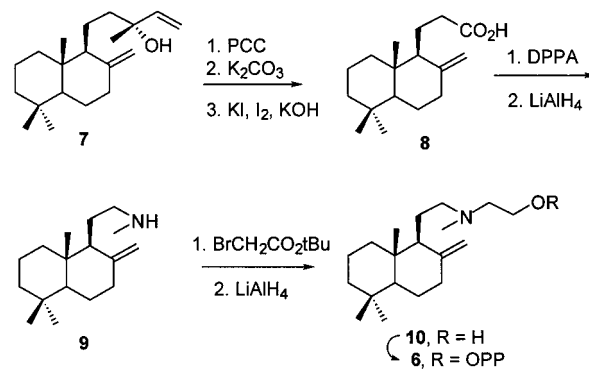
(14) Yamaguchi, S.; Saito, T.; Abe, H.; Yamane, H.; Murofushi, N.; Kamiya, Y. *Plant J.* **1996**, *10*, 101–111.

(15) Davis, E. M.; Croteau, R. In *Topics in Current Chemistry*; Leeper, F., Verderas, J., Eds.; Springer-Verlag: Berlin, 2000; Vol. 209, pp 53–95.

(16) Bohlmann, J.; Meyer-Gauen, G.; Croteau, R. *Proc. Natl. Acad. Sci. U.S.A.* **1998**, *95*, 4126–4133.

(17) Kawaide, H.; Sassa, T.; Kamiya, Y. *J. Biol. Chem.* **2000**, *275*, 2276–2280.

## Scheme 2. Synthesis of 13,14-Dihydro-13-azacopalyl Diphosphate from Manool in Eight Steps



described.<sup>3,9</sup> The preparations of (*E,E,E*)-[1-<sup>3</sup>H]geranylgeranyl diphosphate (120 Ci/mol)<sup>3</sup> and (+)-[1-<sup>3</sup>H]CPP (120 Ci/mol)<sup>4</sup> have been previously described. Kinetic assays with freshly prepared enzyme were performed and the data analyzed as previously described.<sup>4</sup> Micromolar inhibition constants were determined by analysis of the change in *K<sub>M</sub>* upon inclusion of inhibitor. However, because the kinetic assay requires a minimum of 3 nM rAS, it is not possible to satisfy the constraints of the Michaelis–Menten derivation, so determination of nanomolar inhibition constants required use of an alternative experimental protocol. A Dixon-type experiment was utilized in which reaction rates were determined at various inhibitor concentrations in the presence of a fixed concentration of substrate. The relative rates were fitted to a tight binding inhibitor equation<sup>18</sup> to obtain apparent *K<sub>i</sub>*. Acid-catalyzed solvolysis of reaction products was achieved by the addition of HCl to 0.3 M to the reaction mixture, followed by incubation for 15 min at room temperature and pentane extraction.

**Synthesis of 13,14-Dihydro-13-azacopalyl Diphosphate (Scheme 2).** Manool (**7**) was degraded to acid **8** by a three-step literature procedure that involved oxidation (pyridinium chlorochromate, CH<sub>2</sub>-Cl<sub>2</sub>)<sup>19</sup> to a 2:1 mixture of (*E*)- and (*Z*)-copalal followed by a retro-aldol cleavage (K<sub>2</sub>CO<sub>3</sub>, H<sub>2</sub>O/tetrahydrofuran, reflux, 2d, 66% for two steps)<sup>20</sup> and iodoform oxidation of the resulting methyl ketone (KOH, KI, I<sub>2</sub>, 53%). Modified Curtius rearrangement<sup>21</sup> to the isocyanate (diphenylphosphoryl azide, benzene, reflux, 73%) followed by reduction provided methylamine **9** (LiAlH<sub>4</sub>, tetrahydrofuran, reflux and room temperature, 62%), which was alkylated in quantitative yield with *tert*-butyl bromoacetate (tetrahydrofuran, Et<sub>3</sub>N, 0 °C, 96%) and reduced to amino alcohol **10** (LiAlH<sub>4</sub>, Et<sub>2</sub>O, 86%). Conversion to the diphosphate ester followed published procedures developed for the diphosphorylation of 1,2-amino alcohols.<sup>22</sup> Thus, alcohol **10** was converted to the mesylate at low temperatures (mesyl chloride, Et<sub>3</sub>N, CH<sub>2</sub>Cl<sub>2</sub>, –13 °C), followed by displacement with tris(tetabutylammonium) hydrogen pyrophosphate (CH<sub>3</sub>CN, 8.5 h). Counterion exchange on Dowex 50W-X8 (NH<sub>4</sub><sup>+</sup> form) gave a 10:3:1 mixture of ammonium salts containing inorganic pyrophosphate, diphosphate **6**, and an unknown product that exhibited a singlet in the <sup>31</sup>P NMR spectrum. Purification by preparative reverse phase HPLC afforded 13-aza-CPP (**6**, 40% overall yield), which was characterized by its <sup>1</sup>H and <sup>31</sup>P NMR spectra, the latter showing the distinctive pair of doublets associated with monoalkyl diphosphates. The Supporting Information contains a more complete description of the synthetic procedures and characterization data.

**Mutant Construction and Preparation.** Point mutations of rAS were generated by a variation on a previously described polymerase chain reaction (PCR)-based site directed mutagenesis protocol.<sup>23</sup> Two mutated fragments were produced by PCR (40 cycles with annealing

(18) Williams, J. W.; Morrison, J. F. *Methods Enzymol.* **1979**, *63*, 437–467.

(19) Sundararaman, P.; Herz, W. *J. Org. Chem.* **1977**, *42*, 813–819.

(20) Drengler, K. Ph.D. Thesis, University of Illinois, Urbana, 1980.

(21) Ninomiya, K.; Shiori, T.; Yamada, S. *Tetrahedron* **1974**, *30*, 2151–2157.

(22) Steiger, A.; Pyun, H. J.; Coates, R. M. *J. Org. Chem.* **1992**, *57*, 3444–3449.

(23) Shalk, M.; Croteau, R. *Proc. Natl. Acad. Sci. U.S.A.* **2000**, *97*, 11948–11953.

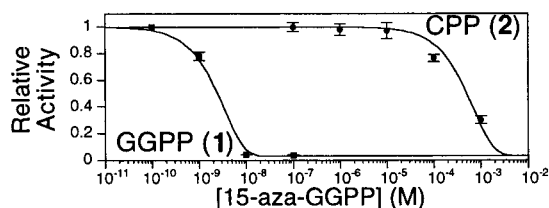


**Figure 1.** Differential inhibition of rAS by 15-aza-GGPP (5) determined at 5  $\mu\text{M}$  GGPP (■) or 3  $\mu\text{M}$  CPP (●). Data are the averages of duplicate assays and the error bars represent the standard deviations.

at 55 °C), using an external 5'-primer (T7 promoter) with a reverse mutagenic primer, and a complementary forward mutagenic primer with an external 3'-primer (T7 terminator). Full-length mutagenized rAS was produced using an overlapping fragment PCR scheme; the fragments overlap in the mutagenic primer region and were joined in an initial unprimed PCR reaction (25 cycles with annealing at 60 °C) and amplified by dilution (1:1000) into a T7 promoter/T7 terminator primed PCR reaction (40 cycles with annealing at 55 °C). *NdeI/BamHI* digestion allowed ligation back into the original expression vector pSBETa.<sup>24</sup> The resulting sequence verified constructs were expressed in *E. coli* BLR and the resulting recombinant enzymes were purified as previously described.<sup>4</sup> The concentration of purified rAS was determined by absorbance at 280 nm using the calculated extinction coefficient ( $138\,350\text{ M}^{-1}\text{ cm}^{-1}$ ).<sup>16</sup>

## Results

**Transition-State Aza Analogues.** To discriminate between possibly discrete active sites responsible for protonation-initiated versus diphosphate ionization-initiated cyclization, we synthesized aza analogues corresponding to carbocation transition state intermediates predicted to occur in the AS-mediated reactions (Scheme 1). Synthesis of 14,15-dihydro-15-azageranylgeranyl diphosphate (15-aza-GGPP, 5) has been previously reported.<sup>25</sup> 13,14-Dihydro-13-azacopalyl diphosphate (13-aza-CPP, 6) was synthesized from manool in eight steps with an overall yield of 5.1% (Scheme 2).

13-Aza-CPP (6) inhibits the rAS-catalyzed (rAS = the recombinant "pseudomature" enzyme of AS) conversion of both [ $^3\text{H}$ ]GGPP ( $K_i^{\text{GGPP}} = 0.5 \pm 0.3\ \mu\text{M}$ ) and [ $^3\text{H}$ ]CPP ( $K_i^{\text{CPP}} = 0.2 \pm 0.05\ \mu\text{M}$ ) to [ $^3\text{H}$ ]abietane olefins to an approximately equal extent. This result is consistent with the AS sequential cyclization mechanism, as 6 is expected to inhibit the second cyclization and thus equally inhibit both reactions, irrespective of the relationship of active sites. In contrast, 15-aza-GGPP (5) mimics the initial carbocation intermediate of the protonation-initiated cyclization and should preferentially inhibit the first reaction. In fact, 5 does inhibit the reaction with GGPP dramatically more effectively than that with (+)-CPP (Figure 1). At concentrations where rAS is completely inhibited (with GGPP as substrate), the reaction with (+)-CPP is unaffected. *The 5 orders of magnitude difference in inhibition ( $K_i^{\text{GGPP}} = 0.25 \pm 0.1\ \text{nM}$ ;  $K_i^{\text{CPP}} = 20 \pm 4\ \mu\text{M}$ ) clearly demonstrates that each cyclization is carried out at individually accessible, and therefore separate, active sites.*

**Site-Directed Mutagenesis of Aspartate-Rich Motifs Defines Active Sites.** To define each active site, PCR site-directed mutagenesis was employed to create point mutants in either aspartate-rich motif thought to be involved in each specific reaction (Scheme 1). Alanine substitution for the second aspartate in the DXDD motif selectively abolishes protonation-initiated cyclization in FCPS/KS<sup>17</sup> and triterpene cyclases.<sup>12</sup> The

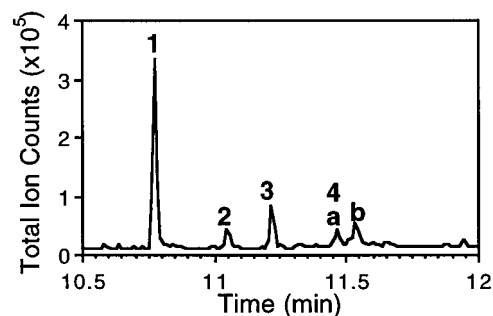


**Figure 2.** GC-MS analysis (total ion chromatogram) of the reaction products (following acid-catalyzed solvolysis) of rAS assayed at 4  $\mu\text{M}$  GGPP under steady-state kinetic conditions. The products indicated are geranylinalool (1, from the rearrangement of GGPP), manool (2, from rearrangement of (+)-CPP), abieta-7(8),13(14)-diene (3, all isomeric olefins rearrange to abieta-7(8),13(14)-diene), and geranylgeraniol (4a (cis-isomer) and 4b (trans-isomer) from solvolysis of GGPP).

corresponding D404A point mutant of rAS exhibits similar behavior in abolishing the conversion of GGPP to (+)-CPP and leaving the reaction of (+)-CPP to products unaffected (see Figure 3a). In a similar fashion, alanine substitution of the first aspartate in the DDXXD motif has been shown to selectively eliminate diphosphate ionization-dependent reactions in FCPS/KS<sup>17</sup> as well as in other terpene synthases.<sup>15</sup> Again, the analogous point mutant of rAS, D621A, selectively eliminates the diphosphate ionization-dependent reaction but not the conversion of GGPP to (+)-CPP (i.e., phosphatase hydrolysis of the reaction product of D621A with GGPP as substrate yields copalol by GC-MS comparison to an authentic sample), which occurs with comparable kinetics to the wild-type enzyme (see Figure 3b). Co-incubation of D404A and D621A with GGPP results in the formation of abietadienes at a rate equal to that of wild-type rAS. Since AS is monomeric (native AS has been previously shown to be monomeric,<sup>3</sup> and gel filtration chromatography (Superdex 200, Pharmacia) indicates that rAS (calculated size = 94 kDa) has a size of  $90 \pm 8\ \text{kDa}$ , demonstrating that the recombinant enzyme is also monomeric), this kinetically effective complementation between mutants defective in the partial reactions suggests that (+)-CPP diffuses freely between the two active sites.

### Detection of Free (+)-CPP in the Steady-State Reaction.

If (+)-CPP freely diffuses between the two active sites of AS, the solution concentration of this intermediate must increase sufficiently to promote productive rebinding at the second active site. Therefore, under steady-state reaction conditions, free (+)-CPP should be detectable in reactions with the wild-type enzyme. For this analysis, acid hydrolysis was utilized both to stop the enzymatic reaction and to hydrolyze the resulting products, which were verified by GC-MS comparison with authentic standards. Free (+)-CPP was easily detectable under kinetic steady-state conditions at low initial concentrations of GGPP (Figure 2). Quantitative analysis further indicated that ~2% of the GGPP had been converted to (+)-CPP under these conditions, representing a 20-fold excess over the amount of rAS present. Failure to detect appreciable amounts of free (+)-CPP at higher initial concentrations of GGPP was instructive; this result indicated that the observed substrate inhibition with GGPP arises from suppression of GGPP cyclization, rather than by GGPP binding to and blocking the second active site as previously suggested (since this would lead to accumulation of (+)-CPP).<sup>4</sup>

**Kinetic Analysis.** Freshly prepared recombinant AS (rAS) was employed for kinetic analyses, which provided  $K_M^{\text{GGPP}} =$

(24) Schenk, P. M.; Baumann, S.; Mattes, R.; Steinbiss, H.-H. *BioTechniques* **1995**, *19*, 196–200.

(25) Ravn, M. M.; Jin, Q.; Coates, R. M. *Eur. J. Org. Chem.* **2000**, 1401–1410.



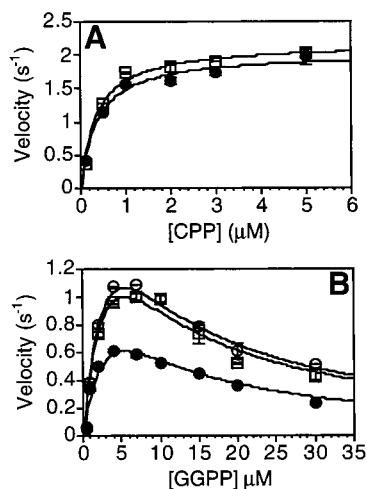


**Figure 3.** Steady-state kinetic analyses of rAS. (A) Comparison of wild-type rAS (●) and D404A (□) with (+)-CPP as substrate. (B) Kinetics for GGPP as substrate with wild-type rAS alone (●) and for wild-type (○) or D621A (□) with saturating concentrations (100 nM) of D404A. Data are the averages of duplicate assays and the error bars represent the standard deviations.

$3 \pm 2 \mu\text{M}$  and  $K_M^{\text{CPP}} = 0.4 \pm 0.2 \mu\text{M}$ ,  $k_{\text{cat}}$  of  $2.2 \pm 0.3 \text{ s}^{-1}$  (for both substrates) and a GGPP substrate inhibition constant ( $K_{\text{si}}$ ) of  $5 \pm 2 \mu\text{M}$  (these kinetic constants differ somewhat from those previously reported<sup>4</sup> due to our earlier failure to appreciate the instability of rAS stored under cryogenic conditions). Although the calculated  $k_{\text{cat}}$  is the same for either substrate, the *observable* reaction rate with GGPP never approaches the level attainable with (+)-CPP due to substrate inhibition as previously noted (Figure 3).<sup>4</sup>

Each active site of AS was independently characterized by the use of the generated mutants that lack one or the other activity. D404A is completely unreactive with GGPP (at least  $10^4$  decrease in  $k_{\text{cat}}$ ) while retaining the ability to react with (+)-CPP. Kinetic analysis of D404A with (+)-CPP revealed essentially identical behavior ( $k_{\text{cat}} = 2.3 \pm 0.2 \text{ s}^{-1}$ ;  $K_M = 0.4 \pm 0.2 \mu\text{M}$ ) to wild-type rAS (Figure 3a), demonstrating a specific role for the DXDD motif in the AS-catalyzed protonation-initiated cyclization reaction. D621A cannot react with (+)-CPP (again at least  $10^4$  decrease in  $k_{\text{cat}}$ ) but clearly cyclizes GGPP to (+)-CPP at kinetically competent rates, as demonstrated by the ability of this mutant to effectively complement the activity of D404A with GGPP as substrate.

The addition of either D404A or D621A to wild-type rAS increased the *observed* overall reaction rate with GGPP as substrate. This seemingly contradictory ability of both mutants to enhance overall catalysis (i.e., with GGPP as substrate) is a consequence of AS containing two separate active sites, coupled with substrate inhibition by GGPP and the free diffusive transfer of the intermediate (+)-CPP. The intrinsic rate-limiting step of the overall reaction resides after the protonation-initiated cyclization of GGPP to (+)-CPP (i.e., the calculated  $k_{\text{cat}}$  for formation of abietadienes is the same for either substrate). However, owing to substrate inhibition, the *observed* reaction rate with GGPP never reaches the maximum rate attainable with (+)-CPP (Figure 3). D621A simply increases the overall reaction rate by converting GGPP to free (+)-CPP, thereby relieving substrate inhibition and allowing the *observed* rate to approach that with (+)-CPP as substrate. Thus, increasing the amount of D621A in the presence of a constant amount of wild-type rAS allows the rate of conversion of GGPP to approach that for an equivalent concentration of (+)-CPP; this enhancement saturates

at  $\sim 100 \text{ nM}$  D621A, just short of the maximum rate obtained with (+)-CPP, and decreases thereafter.

The ability of D404A to increase the observed rate of the overall reaction with GGPP as substrate simply reflects the increased capacity provided by the mutant to utilize excess free (+)-CPP produced by wild-type rAS. Thus, increasing the amount of D404A ultimately exceeds the ability of the first active site (in either wild type or D621A) to produce (+)-CPP. Again, this coupling effect saturates at  $\sim 100 \text{ nM}$  D404A, seemingly just short of the maximum rate. This coupled assay allows approximation of the true rate of the protonation-initiated cyclization as  $k_{\text{cat}} \approx 3 \text{ s}^{-1}$  (Figure 3b), which is  $\sim 35\%$  faster than the rate of the reaction with (+)-CPP and which confirms that the intrinsic rate-limiting step in the overall reaction resides after formation of (+)-CPP. This approach also reveals that D621A exhibits very similar kinetic behavior to wild-type rAS under the same conditions (i.e.,  $K_M \approx 5 \mu\text{M}$  and  $K_{\text{si}} \approx 6 \mu\text{M}$ ; Figure 3b), demonstrating the specific involvement of the DDXD motif in the diphosphate ester ionization step. The coupled assays also exhibit substrate inhibition by GGPP, thereby directly demonstrating that GGPP inhibits its own cyclization. Consistent with this interpretation, the reaction of D404A with (+)-CPP is only weakly inhibited by GGPP, and the inhibition constants for GGPP and 15-aza-GGPP are similar ( $K_i^{\text{CPP}} \sim 23$  and  $\sim 20 \mu\text{M}$ , respectively), and are substantially higher than the observed substrate inhibition constant ( $K_{\text{si}} \sim 5 \mu\text{M}$ ) for the overall reaction. Finally, if GGPP also inhibited the diphosphate ionization-dependent reaction, then (+)-CPP levels would be expected to increase with time, resulting in a reaction rate increase that is contrary to the observed kinetic behavior.

## Discussion

Bifunctional abietadiene synthase catalyzes two sequential cyclization reactions to produce a mixture of abietadiene isomers (Scheme 1).<sup>4</sup> Protonation-initiated cyclization of the universal diterpene precursor GGPP generates the stable bicyclic intermediate (+)-CPP, which further undergoes diphosphate ester ionization-initiated cyclization to a sandaracopimarenyl intermediate that, via intramolecular proton transfer, is coupled to a 1,2-methyl migration;<sup>7,8</sup> several alternative deprotonations then yield the final mixture of products. The selective inhibition displayed by the transition-state analogue 15-aza-GGPP (Scheme 1, 5), corresponding to the first carbocationic intermediate of the catalytic cycle, demonstrated that each cyclization reaction is carried out at a separate active site. Thus, at concentrations of 5 where the cyclization of GGPP is completely inhibited, (+)-CPP is readily converted to abietadienes (Figure 1), clearly demonstrating the distinct nature of the two active sites.

The potent inhibition by 15-aza-GGPP (5) indicates a large increase in the affinity for this transition-state analogue relative to the substrate GGPP ( $K_M/K_i \approx 10^4$ ,  $\Delta\Delta G^\ddagger = 5.5 \text{ kcal/mol}$ ), consistent with transition-state stabilization by AS in the protonation-initiated reaction. The magnitude of this effect approximates that reported for inhibition by a similar transition-state analogue (2-(dimethylamino)ethyl diphosphate) of isopentenyl diphosphate isomerase, which also catalyzes a protonation-initiated reaction.<sup>26,27</sup> It is noteworthy that 5 is a much more potent inhibitor than any of the numerous transition-state analogues evaluated to date with triterpene cyclases which catalyze similar protonation-initiated cyclization reactions, and

(26) Reardon, J. E.; Abeles, R. H. *Biochemistry* **1986**, *25*, 5609–5616.  
(27) Muehlbacher, M.; Poulter, C. D. *Biochemistry* **1988**, *27*, 7315–7328.

		DXDD	DDXXD
T.S.	"Insertion"	N-terminal domain	C-terminal "catalytic" domain

**Figure 4.** Structural schematic of AS, as modeled from 5-*epi*-aristolochene synthase,<sup>28</sup> illustrating the locations of the aspartate-rich motifs, transit sequence (T.S.), and the unusual insertion element that is also found in a few other terpenoid synthases.<sup>16</sup>

which also contain a catalytically important DXDD motif.<sup>12,13</sup> In contrast, the inhibition exhibited by 13-aza-CPP (**6**) on the conversion of CPP to abietadienes is essentially the same as the binding affinity of (+)-CPP ( $K_M^{CPP}/K_I^{CPP} = 2$ ). This bicyclic aminodiphosphate (**6**) behaves as an inert substrate mimic rather than as a true transition-state analogue.

The involvement of two distinct active sites in bifunctional AS of grand fir is similar to the arrangement of active sites in the bifunctional kaurene synthase of fungal origin<sup>10,17</sup> and reminiscent of the requirement for two separate enzymes in the production of (–)-kaurene in higher plants.<sup>5,6</sup> However, in contrast to the observed channeling of the (–)-CPP intermediate in the biosynthesis of kaurene by these enzymes,<sup>5,6,17</sup> the (+)-CPP intermediate of AS freely diffuses between active sites. This latter phenomenon was initially suggested by the surprising finding that mutants specifically lacking in one or the other cyclization activity could effectively complement each other with GGPP as substrate, and was confirmed by the demonstration of excess free (+)-CPP intermediate under steady-state kinetic conditions (Figure 2).

The two aspartate-rich motifs of AS were previously suggested to be involved in the two cyclization reactions catalyzed,<sup>4,9</sup> based upon the occurrence of similar sequence elements in mechanistically related terpenoid synthases.<sup>12,13,15</sup> Mutations in each aspartate cluster confirmed the specific requirement for each in one of the two cyclizations catalyzed by AS. Sequence alignments<sup>16</sup> and comparison to the crystal structure of 5-*epi*-aristolochene synthase<sup>28</sup> indicate that the two active sites of AS occur in structurally distinct domains (Figure 4). Since the active site of most terpenoid synthases is considered to reside primarily in the C-terminal domain, the present results with AS provide an additional role<sup>29</sup> for the N-terminal (glycosyl hydrolase-like) domain that is found in all plant terpene synthases, although its function is largely unknown. These structural and functional observations with AS may be of evolutionary significance because AS appears to be a close relative of the ancestral plant terpenoid synthase based upon both protein sequence phylogeny<sup>16</sup> and genomic organization.<sup>30</sup> Thus, while the N-terminal, glycosyl hydrolyase-like, domain is of functional utility in the seemingly ancient AS, its retention in other plant terpenoid synthase family members may be largely relectual.

A number of lines of evidence have been presented to demonstrate that GGPP inhibits its own cyclization, resulting

(28) Starks, C. M.; Back, K.; Chappell, J.; Noel, J. P. *Science* **1997**, *277*, 1815–1820.

(29) Williams, D. C.; McGarvey, D. J.; Katahira, E. J.; Croteau, R. *Biochemistry* **1998**, *37*, 12213–12220.

(30) Trapp, S. C.; Croteau, R. B. *Genetics* **2001**, *158*, 811–832.

in the observed overall rate suppression. First, the steady-state concentration of free (+)-CPP decreases with increasing concentrations of GGPP and parallels the observed rate decrease for the overall reaction. If GGPP inhibited the overall reaction by binding at the second active site, then (+)-CPP would be expected to accumulate over time. As an additional consequence, such accumulation would result in the reaction rate increasing with time as GGPP concentrations decreased and inhibition was relieved; such kinetic behavior was not observed. Second, GGPP and the 15-aza-GGPP analogue only weakly inhibit the reaction of AS with (+)-CPP, at a concentration much higher ( $K_i \sim 20 \mu\text{M}$ ) than that observed for substrate inhibition of the overall reaction ( $K_{si} \sim 5 \mu\text{M}$ ). Third, kinetic analysis of the cyclization of GGPP, utilizing a coupled assay approach with the mutant enzyme (D404A) deficient in this reaction, directly demonstrated that GGPP inhibition arises from interaction at the first active site (Figure 3b).

## Conclusions

The potent selective inhibition exhibited by the transition-state analogue, 15-aza-GGPP, demonstrated that abietadiene synthase carries out the two sequential, mechanistically distinct reactions at separate active sites. The tight binding of 15-aza-GGPP strongly indicates a role for transition-state stabilization in the protonation-initiated (first) cyclization step. Surprisingly, it was found that the (+)-CPP intermediate of the reaction scheme is not channeled within this monomeric enzyme, but freely diffuses between the two active sites. Mutational analysis of the two aspartate-rich motifs has specifically defined the two active sites and indicated that they are contained in structurally distinct domains. Kinetic analysis with these mutants verified that the intrinsic rate-limiting step in the overall reaction resides after formation of (+)-CPP and demonstrated that GGPP inhibits its own cyclization. Thus, AS binds GGPP at an active site, in part defined by the DXDD motif, in the N-terminal domain where it undergoes protonation-initiated cyclization to form (+)-CPP. This intermediate must then diffuse out of this active site and rebind at a distinct second active site, in part defined by the DDXXD motif, in the C-terminal domain (either of the same or a different molecule of AS). At this site, diphosphate ester ionization initiates the second cyclization and the reaction cycle is completed to yield the olefinic products.

**Acknowledgment.** This work was supported by National Institutes of Health Grants GM31354 to R.B.C. and GM13956 to R.M.C., and by a Postdoctoral Fellowship from the Jane Coffin Childs Memorial Fund for Medical Research to R.J.P. We thank C. Burke for performing size analysis of rAS by gel filtration chromatography.

**Supporting Information Available:** Experimental details of 13,14-dihydro-13-azacopalyl diphosphate synthesis (PDF). This material is available free of charge via the Internet at <http://pubs.acs.org>.

JA010670K